

TWO DIMENSIONAL DYNAMIC ANALYSIS OF METAL HYDRIDE HYDROGEN ENERGY STORAGE CONDUCTION BED MODELS

M.A. El-Osairy

Dept. of Eng. Math. and Phys.,
Alexandria University,
Alexandria, Egypt.

I.A. El-Osery

Nuclear Power Plant Authority,
P.O. Box 108, Abbassia,
Cairo, Egypt.

A.M. Metwally

Nuclear Eng. Dept.,
Alexandria University,
Alexandria, Egypt.

Mayssa A. Hassan

Department of Eng. Math. and Phys.,
Alexandria University, Egypt.

ABSTRACT

This study discusses the problems of mass and heat transfer in metal hydride storage beds through the conduction bed model. Energy and mass equations were solved numerically in two dimensions by the use of the alternating direction implicit method. A computer code was adapted and revised to deal with different geometries and flow regimes. The case of LaNi_5H_6 metal hydride, with water as working fluid, was treated and the results on temperature and composition distributions are provided and discussed.

NOMENCLATURE

A_f	Wetted surface area of the bed, cm^2	P_x	Dimensionless radial pitch
C_f	Fluid heat capacity, $\text{cal./gm.}^\circ\text{C}$	P_y	Dimensionless axial pitch
C_s	Solid heat capacity, $\text{cal./gm.}^\circ\text{C}$	Q	Heat of reaction per unit hydrogen mass, cal./gm H_2
D_H	Hydraulic diameter, cm	R	Reaction rate, $\text{gm H}_2/\text{sec. cm}^3$
H	Height of the bed, cm	r	Radial distance, cm
h	Heat transfer coefficient, $\text{cal./sec.}^\circ\text{C. cm}^2$	r_i	Rod inside radius, cm
i	Index indicating radial node number	r_o	Rod outside radius, cm
j	Index indicating axial node number	r_{of}	Outside radius of the fluid flow, cm
K	Effective bed thermal conductivity, $\text{cal./}^\circ\text{C.cm. sec}$	T	Solid temperature, $^\circ\text{C}$
K_f	Fluid thermal conductivity, $\text{cal./sec. cm}^\circ\text{C}$	t	Time, sec
M	Total number of axial nodes	T_{fE}	Exit fluid temperature, $^\circ\text{C}$
MW	Molecular weight of metal hydride divided by number of metal atoms per molecule of hydride, gm/gm mole	T_{fI}	Inlet fluid temperature, $^\circ\text{C}$
\dot{m}	Fluid mass flux, gm/sec. cm^2	T_{fi}	Fluid temperature at the bed inner surface, $^\circ\text{C}$
\dot{m}_f	Fluid mass flow rate, gm/sec	T_{fo}	Fluid temperature at the bed outer surface, $^\circ\text{C}$
m_i	Radial mesh ratio, dimensionless	T_I	Initial bed temperature, $^\circ\text{C}$
m_j	Axial mesh ratio, dimensionless	z	Axial distance, cm
N	Total number of radial nodes	ρ_s	Solid density, gm/cm^3
n	Index indicating discrete time coordinate	ϵ	Bed void fraction (free-to-total volume ratio)
P_b	Bed hydrogen pressure, atm.	ξ	Hydrogen-to-metal atom ratio (H/M)
P_D	Equilibrium dissociation pressure, atm.	μ_f	Fluid viscosity, gm/sec. cm
$-P_v$	Dimensionless time increment	α_1, α_2	Constants each of them equals 0 for zero-temperature gradient boundary condition (insulated boundary) or equals 1 for convective boundary condition
		β	Constant equals 1 or 0 for rectangular plate

- γ or cylindrical geometry respectively
- γ Geometric selection parameter equals 0 for rectangular plate or 1 for cylindrical geometry
- γ_1 Configuration selection parameter equals 0 for one dimensional problem or 1 for two dimensional problem

1. INTRODUCTION

Many recent studies have cleared that chemical energy storage offers promising potentials in connection with today's energy transmission, distribution, and utilization systems. One of the most attractive chemical energy storage techniques is hydrogen energy storage [1]. Hydrogen can be stored as gaseous, liquid, or metal hydride. Hydrogen storage as metal hydrides is gaining more attention as it has the merits of high volumetric hydrogen density as well as safe handling and long term stability without refrigeration requirements.

The purpose of this study is to predict the two-dimensional time dependent temperature and hydrogen reaction rate distributions in metal hydride storage beds based on the conduction bed model [2]. A computer code called "TOBAM" [3] was adapted and revised to allow the use of a variety of bed geometries and flow regimes.

2. MATHEMATICAL MODEL

The problem under discussion can be explained physically as a two-dimensional unsteady heat generation (or absorption) problem when the heat source (or sink) is time and composition dependent. For rectangular plate (or cylindrical) configuration under fixed physical and operating conditions, the general formula of space-time dependent energy balance equation can be written as:

$$K \frac{\partial^2 T}{\partial r^2} + \frac{\gamma K}{r} \frac{\partial T}{\partial r} + \gamma_1 K \frac{\partial^2 T}{\partial z^2} - (1 - \epsilon) R Q = (1 - \epsilon) \rho_s C_s \frac{\partial T}{\partial t} \quad (1)$$

the associated mass balance equation is given by:

$$\frac{\partial \xi}{\partial t} = - \frac{MW}{\rho_s} R \quad (2)$$

The reaction rate "R" is considered linearly dependent on the hydrogen fraction being completely reacted and the hydrogen pressure, while it is considered exponentially dependent on hydride temperature. Thus, it can be represented as:

$$R = f_1(\xi, P, T) = \frac{\xi - \xi_F}{\xi_I - \xi_F} * \frac{P_D - P_b}{P_D} * A_1 \exp \left[\frac{-A_2}{T + 273} \right] \quad (3)$$

where

$$P_D = f_2(T) = \exp \left[\frac{A}{T + 273} + B \right] \quad (4)$$

and A_1, A_2, A and B are metal hydride specific constants.

The energy and mass balance equations are to be solved under the initial conditions:

$$\left. \begin{aligned} T(r, z, 0) &= T_I \\ \xi(r, z, 0) &= \xi_I \end{aligned} \right\} \text{for } r_1 \leq r \leq r_o, 0 \leq z \leq H. \quad (5)$$

Table (1) shows the different boundary condition alternatives [3]. For the most practical applications the proposed boundary condition alternative is the CCTT-alternative, so it is considered in this work. The energy balance for the fluid can be written as [4]:

$$\frac{\dot{m}_f C_f H}{h A_f} \frac{\partial T_f}{\partial z} = T - T_f \quad (6)$$

and the heat transfer coefficient can be calculated using the correlation [2]:

$$h = \left[\frac{0.023 K_f}{D_H} \right] \left[\frac{D_H \dot{m}}{\mu_f} \right]^{0.8} \left[\frac{\mu_f C_f}{K_f} \right]^{0.4} \quad (7)$$

3. NUMERICAL SOLUTION

The first step of numerical solution is to transform the mathematical formulation into a dimensionless form. Then a discrete form of the problem is developed using the Alternating Direction Implicit (ADI) method [5].

The dimensionless parameters are considered as:

Table 1. Boundary Condition Alternatives.

CCTT-alternative	CCII-alternative	CCCC-alternative
$k \frac{\partial T}{\partial r} = \alpha_1 h_i [T - T_{fi}] ; r=r_i$	$K \frac{\partial T}{\partial r} = h_i [T - T_{fi}] ; r=r_i$	$K \frac{\partial T}{\partial r} = h_i [T - T_{fi}] ; r=r_i$
$k \frac{\partial T}{\partial r} = -\alpha_2 h_o [T - T_{fo}] ; r=r_o$	$K \frac{\partial T}{\partial r} = -h_o [T - T_{fo}] ; r=r_o$	$K \frac{\partial T}{\partial r} = -h_o [T - T_{fo}] ; r=r_o$
$T = T_{fi} ; z = 0$	$\frac{\partial T}{\partial z} = 0 ; z = 0$	$K \frac{\partial T}{\partial z} = h_d [T - T_{fi}] ; z = 0$
$T = T_{fe} ; z = H$	$\frac{\partial T}{\partial z} = 0 ; z = H$	$K \frac{\partial T}{\partial z} = -h_u [T - T_{fe}] ; z = H$

$$X = \frac{(r - r_i)}{(r_o - r_i)} \quad (8)$$

$$Y = \frac{z}{H} \quad (9)$$

$$u = \frac{T - T_{fi}}{T_I - T_{fi}} \quad (10)$$

$$w = (\xi - \xi_F) / (\xi_I - \xi_F) \quad (11)$$

$$v = \theta_1 t \quad (12)$$

$$u_f = (T_f - T_{fi}) / (T_I - T_{fi}) \quad (13)$$

Thus, the dimensionless formulae of energy and mass balance equations can be written as:

$$\frac{\partial^2 u}{\partial X^2} + \frac{\gamma}{r_c + X} \frac{\partial u}{\partial X} + \gamma_1 \theta_5 \frac{\partial^2 u}{\partial Y^2} - q \frac{\partial w}{\partial v} = \frac{\partial u}{\partial v} \quad (14)$$

$$\frac{\partial w}{\partial v} = -\theta_2 w f(u) \quad (15)$$

where

$$f(u) = \frac{P_D(u) - P_b}{P_D(u)} \cdot \exp \left[-\frac{A_2}{(T_I - T_{fi}) + u + T_{fi} + 273} \right] \quad (16)$$

with the initial conditions:

$$u(X, Y, 0) = 1; 0 \leq X \leq 1, 0 \leq Y \leq 1 \quad (17)$$

$$w(X, Y, 0) = 1; 0 \leq X \leq 1, 0 \leq Y \leq 1 \quad (18)$$

and with the boundary conditions (CCTT - alternative)

$$\frac{\partial u(0, Y, v)}{\partial X} = \alpha_1 \theta_3 \left[u(0, Y, v) - \frac{T_a(Y, v) - T_{fi}}{T_I - T_{fi}} \right]; v > 0, 0 \leq Y \leq 1 \quad (19)$$

$$\frac{\partial u(1, Y, v)}{\partial X} = -\alpha_2 \theta_4 \left[u(1, Y, v) - \frac{T_b(Y, v) - T_{fi}}{T_I - T_{fi}} \right]; v > 0, 0 \leq Y \leq 1 \quad (20)$$

$$u(X, 0, v) = 0; v > 0, 0 \leq X \leq 1 \quad (21)$$

$$u(X, 1, v) = \frac{T_{fe} - T_{fi}}{T_I - T_{fi}}; v > 0, 0 \leq X \leq 1 \quad (22)$$

where the constants which present in the above equations can be defined as:

$$r_c = r_i / (r_o - r_i) \quad (23)$$

$$q = \frac{-Q(\xi_I - \xi_F)}{C_s (T_I - T_{fi}) (MW)} \quad (24)$$

$$\theta_1 = K / [(1 - \epsilon)(r_o - r_i)^2 \rho_s C_s] \quad (25)$$

$$\theta_2 = \frac{A_1 C_s (1 - \epsilon) (r_o - r_i)^2}{K(\xi_I - \xi_F)} (MW) \quad (26)$$

$$\theta_3 = h_i (r_o - r_i) / K \quad (27)$$

$$\theta_4 = h_o (r_o - r_i) / K \quad (28)$$

$$\theta_5 = (r_o - r_i)^2 / H^2 \quad (29)$$

The dimensionless formulation of the fluid energy equation can be written as:
for outer flow:

$$\frac{\partial u_f}{\partial Y} = \beta_o [u(1, Y) - u_f(Y)]; 0 \leq Y \leq 1 \quad (30)$$

and for inner flow:

$$\frac{\partial u_f}{\partial Y} = \beta_i [u(0, Y) - u_f(Y)]; 0 \leq Y \leq 1 \quad (31)$$

where for rectangular plate geometry

$$\beta_o = 2h_o / [\dot{m} C_f (r_{of} - r_o)] \quad \text{and} \quad \beta_i = 0 \quad (32)$$

and for cylindrical geometry

$$\beta_o = 2r_o h_o / [\dot{m} C_f (r_{of}^2 - r_o^2)] \quad \text{and} \quad \beta_i = (2h_i) / (\dot{m} C_f r_i) \quad (33)$$

The problem in its dimensionless form is completely defined. A discrete form of this problem is developed using the (ADI) method. The main idea in this method is to use two difference equations successively through which the time step is always half the time increment. There will be two finite difference equations for energy balance equation, the first is implicit only in the X-direction while the second is implicit only in the Y-direction.

Accordingly, the open integration domain defined by $0 \leq X \leq 1$, $0 \leq Y \leq 1$, and $v > 0$ is replaced by a net whose nodal points are denoted by:

$$X_i = (i - 1) P_x; \quad i = 1, 2, \dots, N \quad (34)$$

$$Y_j = (j - 1) P_y; \quad j = 1, 2, \dots, M \quad (35)$$

$$v_n = (n - 1) P_v; \quad n = 1, 2, 3, \dots \quad (36)$$

where $P_x = 1/(N - 1)$ and $P_y = 1/(M - 1)$. Applying the (ADI) method, the energy balance equation can be written as:

$$\frac{U_{i,j}^{n+1/2} - U_{i,j}^n}{P_x/2} = \frac{1}{P_x^2} [U_{i-1,j}^{n+1/2} - 2U_{i,j}^{n+1/2} + U_{i+1,j}^{n+1/2}] + \frac{\gamma}{(i-1)P_x + r_c} \cdot \frac{1}{2P_x} [U_{i-1,j}^{n+1/2} - U_{i-1,j}^n] + \frac{\gamma \theta_5}{P_y^2} [U_{i,j-1}^n - 2U_{i,j}^n + U_{i,j+1}^n] - \frac{q}{P_x/2} [W_{i,j}^{n+1/2} - W_{i,j}^n] \quad (37)$$

followed by

$$\frac{U_{i,j}^{n+1} - U_{i,j}^{n+1/2}}{P_y/2} = \frac{1}{P_y^2} [U_{i,j-1}^{n+1/2} - 2U_{i,j}^{n+1/2} + U_{i,j+1}^{n+1/2}] + \frac{\gamma}{(i-1)P_x + r_c} \cdot \frac{1}{2P_x} [U_{i-1,j}^{n+1/2} - U_{i-1,j}^n] + \frac{\gamma_1 \theta_5}{P_y^2} [U_{i,j-1}^{n+1} - 2U_{i,j}^{n+1} + U_{i,j+1}^{n+1}] - \frac{q}{P_y/2} [W_{i,j}^{n+1} - W_{i,j}^{n+1/2}] \quad (38)$$

where $U_{i,j}^{n+1/2}$ and $W_{i,j}^{n+1/2}$ are intermediate values at the end of the first time step.

The discrete form of mass balance equation is developed through the application of Picard's approximation [6] and the result can be written as:

$$W_{i,j}^{n+1} = W_{i,j}^n \exp[-\theta_2 f(U_{i,j}^n) P_v] \quad (39)$$

Thus, the finite difference energy equations can be written as:

$$-a_{i,j} U_{i-1,j}^{n+1/2} + b_{i,j} U_{i,j}^{n+1/2} - e_{i,j} U_{i+1,j}^{n+1/2} = c_{i,j} U_{i,j-1}^n + f_{i,j} U_{i,j}^n + d_{i,j} U_{i,j+1}^n + Z_{i,j}^n \quad (40)$$

followed by

$$-C_{i,j} U_{i,j-1}^{n+1} + g_{i,j} U_{i,j}^{n+1} - D_{i,j} U_{i,j+1}^{n+1} = G_{i,j} U_{i-1,j}^{n+1/2} + F_{i,j} U_{i,j}^{n+1/2} + E_{i,j} U_{i+1,j}^{n+1/2} + Z_{i,j}^{n+1/2} \quad (41)$$

where

$$Z_{i,j}^n = \frac{2q}{m_i} (W_{i,j}^n - W_{i,j}^{n+1/2}) \quad (42)$$

$$Z_{i,j}^{n+1/2} = \frac{2q}{\theta_5 m_j} (W_{i,j}^{n+1/2} - W_{i,j}^{n+1}) \quad (43)$$

$$m_i = P_v / P_x^2 \quad (44)$$

Table 2. Coefficients of equation (40)

Coefficient	Expression	Regime
$a_{i,j}$	0	$i = 1$
$b_{i,j}$	$2(1 + \frac{1}{m_i}) + 2\alpha_1 \theta_3 P_x \left[1 - \frac{0.5\gamma P_x}{\beta + r_c} \right]$	$2 \leq j \leq M-1$
$e_{i,j}$	2	
$a_{i,j}$	$1 - \frac{0.5\gamma}{i - 1 + r_c / P_x}$	$2 \leq i \leq N-1$
$b_{i,j}$	$2(1 + \frac{1}{m_i})$	$2 \leq j \leq M-1$
$e_{i,j}$	$1 + \frac{0.5\gamma}{i - 1 + r_c / P_x}$	
$a_{i,j}$	2	$i = N$
$b_{i,j}$	$2(1 + \frac{1}{m_i}) + 2\alpha_2 \theta_4 P_x \left[1 + \frac{0.5\gamma P_x}{1 + r_c} \right]$	$2 \leq j \leq M-1$
$e_{i,j}$	0	
$c_{i,j}$	0	$1 \leq i \leq N$
$f_{i,j}$	$2(\frac{1}{m_i} - \gamma_1 \theta_5 \lambda)$	$j = 2$
$d_{i,j}$	$\gamma_1 \theta_5 \lambda$	
$c_{i,j}$	$\gamma_1 \theta_5 \lambda$	$1 \leq i \leq N$
$f_{i,j}$	$2(\frac{1}{m_i} - \gamma_1 \theta_5 \lambda)$	
$d_{i,j}$	$\gamma_1 \theta_5 \lambda$	$3 \leq j \leq M-2$
$c_{i,j}$	$\gamma_1 \theta_5 \lambda$	$1 \leq i \leq N$
$f_{i,j}$	$2(\frac{1}{m_i} - \gamma_1 \theta_5 \lambda)$	
$d_{i,j}$	0	$j = M-1$

Table 2. Cont.

Coefficient	Expression	Regime
$Z_{i,j}^n$	$Z_{i,j}^n + 2\alpha_1 \theta_3 P_x \left[1 - \frac{0.5 \gamma P_x}{\beta + r_c} \right] \left[\frac{T_{fi(j)} - T_{fl}}{T_I - T_{fl}} \right]$	$1 < j < M-1$; $i = 1$
$Z_{i,j}^n$	$Z_{i,j}^n$; $2 \leq i \leq N-1$
$Z_{i,j}^n$	$Z_{i,j}^n + 2\alpha_2 \theta_4 P_x \left[1 + \frac{0.5 \gamma P_x}{1 + r_c} \right] \left[\frac{T_{fo(j)} - T_{fl}}{T_I - T_{fl}} \right]$; $i = N$
$Z_{i,j}^n$	$Z_{ij}^n + 2\alpha_1 \theta_3 P_x \left[1 - \frac{0.5 \gamma P_x}{\beta + r_c} \right] \left[\frac{T_{fi(M-1)} - T_{fl}}{T_I - T_{fl}} \right]$ $+ \gamma_1 \theta_5 \lambda \left[\frac{T_{fo(M)} - T_{fl}}{T_I - T_{fl}} \right]$	$j = M - 1$; $i = 1$
$Z_{i,j}^n$	$Z_{ij}^n + \gamma_1 \theta_5 \lambda \left[\frac{T_{fo(M)} - T_{fl}}{T_I - T_{fl}} \right]$; $2 \leq i \leq N-1$
$Z_{i,j}^n$	$Z_{ij}^n + 2\alpha_2 \theta_4 P_x \left[1 + \frac{0.5 \gamma P_x}{1 + r_c} \right] \left[\frac{T_{fo(M-1)} - T_{fl}}{T_I - T_{fl}} \right]$ $+ \gamma_1 \theta_5 \lambda \left[\frac{T_{fo(M)} - T_{fl}}{T_I - T_{fl}} \right]$; $i = N$

where : $\lambda = m_j/m_i$

Table 3. Coefficients of equation (41)

Coefficient	Expression	Regime
$C_{i,j}$ $g_{i,j}$ $D_{i,j}$	0 $2\left(\gamma_1 + \frac{1}{\theta_5 m_j}\right)$ γ_1	$j = 2$ $1 \leq i \leq N$
$C_{i,j}$ $g_{i,j}$ $D_{i,j}$	γ_1 $2\left(\gamma_1 + \frac{1}{\theta_5 m_j}\right)$ γ_1	$3 \leq j \leq M-2$ $1 \leq i \leq N$
$C_{i,j}$ $g_{i,j}$ $D_{i,j}$	γ_1 $2\left(\gamma_1 + \frac{1}{\theta_5 m_j}\right)$ 0	$j = M - 1$ $1 \leq i \leq N$
$G_{i,j}$ $F_{i,j}$ $E_{i,j}$	0 $2\left(\frac{1}{\theta_5 m_j} - \frac{1}{\theta_5 \lambda}\right) - \frac{2\alpha_1 \theta_3 P_x}{\theta_5 \lambda} \left[1 - \frac{0.5\gamma P_x}{\beta + r_c} \right]$ $\frac{2}{\lambda \theta_5}$	$i = 1$ $2 \leq j \leq M-1$
$G_{i,j}$ $F_{i,j}$ $E_{i,j}$	$\frac{1}{\theta_5 \lambda} \left[1 - \frac{0.5\gamma}{i - 1 + r_c / P_x} \right]$ $2 \left[\frac{1}{\theta_5 m_j} - \frac{1}{\theta_5 \lambda} \right]$ $\frac{1}{\theta_5 \lambda} \left[1 + \frac{0.5\gamma}{i - 1 + r_c / P_x} \right]$	$2 \leq i \leq N-1$ $2 \leq j \leq M-1$
$G_{i,j}$ $F_{i,j}$ $E_{i,j}$	$\frac{2}{\theta_5 \lambda}$ $2 \left[\frac{1}{\theta_5 m_j} - \frac{1}{\theta_5 \lambda} \right] - \frac{2\alpha_2 \theta_4 P_x}{\theta_5 \lambda} \left[1 + \frac{0.5\gamma P_x}{1 + r_c} \right]$ 0	$i = N$ $2 \leq j \leq M-1$

Table 3. Cont.

Coefficient	Expression	Regime
$Z_{i,j}^{n+\frac{1}{2}}$	$Z_{i,j}^{n+\frac{1}{2}} + \frac{2\alpha_1\theta_3P_x}{\theta_5\lambda} \left[1 - \frac{0.5\gamma P_x}{\beta + r_c} \right] \left[\frac{T_{fi}(j) - T_{ff}}{T_I - T_{ff}} \right]$	$i = 1$; $2 \leq j \leq M-2$
$Z_{i,j}^{n+\frac{1}{2}}$	$Z_{i,j}^{n+\frac{1}{2}} + \frac{2\alpha_1\theta_3P_x}{\theta_5\lambda} \left[1 - \frac{0.5\gamma P_x}{\beta + r_c} \right] \left[\frac{T_{fi}(M-1) - T_{ff}}{T_I - T_{ff}} \right]$ $+ \gamma_1 \frac{T_{fo}(M) - T_{ff}}{T_I - T_{ff}}$; $j = M-1$
$Z_{i,j}^{n+\frac{1}{2}}$	$Z_{i,j}^{n+\frac{1}{2}}$	$1 < i < N$; $2 \leq j \leq M-2$
$Z_{i,j}^{n+\frac{1}{2}}$	$Z_{i,j}^{n+\frac{1}{2}} + \gamma_1 \left[\frac{T_{fo}(M) - T_{ff}}{T_I - T_{ff}} \right]$; $j = M - 1$
$Z_{i,j}^{n+\frac{1}{2}}$	$Z_{i,j}^{n+\frac{1}{2}} + \frac{2\alpha_2\theta_4P_x}{\theta_5\lambda} \left[1 + \frac{0.5\gamma P_x}{1 + r_c} \right] \left[\frac{T_{fo}(j) - T_{ff}}{T_I - T_{ff}} \right]$	$i = N$; $2 \leq j \leq M-2$
$Z_{i,j}^{n+\frac{1}{2}}$	$Z_{i,j}^{n+\frac{1}{2}} + \frac{2\alpha_2\theta_4P_x}{\theta_5\lambda} \left[1 + \frac{0.5\gamma P_x}{1 + r_c} \right] \left[\frac{T_{fo}(j) - T_{ff}}{T_I - T_{ff}} \right]$ $+ \gamma_1 \frac{T_{fo}(M) - T_{ff}}{T_I - T_{ff}}$; $j = M-1$

and

$$m_j = P_v/P_y^2 \quad (45)$$

The coefficients of equations (40) and (41) are listed in Tables (2) and (3).

The finite difference approximation of the initial conditions leads to:

$$U^1_{i,j} = 1; 1 \leq i \leq N, 1 \leq j \leq M \quad (46)$$

$$W^1_{i,j} = 1; 1 \leq i \leq N, 1 \leq j \leq M \quad (47)$$

The finite difference approximation of the boundary condition for CCTT-alternative leads to:

$$U^a_{0,j} = U^a_{2,j} - 2\alpha_1 \theta_3 P_x \left[U^a_{1,j} - \frac{T_{fl}(j) - T_{fl}}{T_1 - T_{fl}} \right]; n > 1, 2 \leq j \leq M \quad (48)$$

$$U^a_{N-1,j} = U^a_{N-1,j} - 2\alpha_2 \theta_4 P_x \left[U^a_{N,j} - \frac{T_{fo}(j) - T_{fl}}{T_1 - T_{fl}} \right]; n > 1, 2 \leq j \leq M \quad (49)$$

$$U^a_{i,1} = 0; n > 1, 1 \leq i \leq N \quad (50)$$

$$U^a_{i,M} = \frac{T_{fo}(M) - T_{fl}}{T_1 - T_{fl}}; n > 1, 1 \leq i \leq N \quad (51)$$

Finally, the finite difference approximation of the fluid temperature equations can be written as;

For inner flow

$$UF_{j+1} = [1 - HP_y \beta_i] UF_j + HP_y \beta_i U_{1,j} \quad (52)$$

For outer flow

$$UF_{j+1} = [1 - H P_y \beta_o] UF_j + HP_y \beta_o U_{N,j} \quad (53)$$

The numerical solution of the problem using the ADI method is defined by equations (40), (41), (42), (43) and (39) whose solutions give the space-time nodal values of temperature and hydrogen-to-metal atom ratio (H/M).

4. CASE STUDY, RESULTS AND DISCUSSIONS

The computer code "TOBAM" is used to study and analyse the process of discharging hydrogen from LaNi₅H₆ metal hydride storage bed. The bed is composed of multiple of hollow cylinders of LaNi₅H₆

metal hydride with water flowing inside the cylinders as well as over the outer surfaces. The physical and operating conditions [7] are presented in Table (4).

Table 4. Physical and Operating Conditions.

Item	value
Initial bed temperature, °C	10.0
Reaction temperature (T _R), °C	12.7
Inlet fluid temperature (T _{fl}), °C	80.0
Bed effective thermal conductivity cal/cm.°C. sec	0.003152
Solid heat capacity, cal./gm °C	0.1366
Solid density, gm/cm ³	6.59
Bed void fraction	0.4
Heat of reaction per unit mass of hydrogen, cal/gmH ₂	3701.94
Bed hydrogen pressure, atm.	1.0
Initial hydrogen-to-metal atom ratio (ξ _i)	1.0
Final hydrogen-to-metal atom ratio (ξ _f)	0.05
Water mass flux, gm/cm ² . sec	10.0
Cylinder outer radius, cm	11.0
Cylinder inner radius, cm	1.0
Cylinder height, cm	11.11

Figure (1) presents the radial temperature distribution at 90 minutes discharging time and different dimensionless axial distances. The concaved shape of the temperature profile is due to the endothermic dehydrating reaction feature of used metal hydride in dehydrating phase. As expected, the axial temperature is maximum at the inner and outer surfaces (X=0, X=1) where the working fluid is in a direct contact with those surfaces. The radial temperature distributions are asymmetrical (minimum at about X=0.4) due to the fact that the heat transfer areas perpendicular to the radius are not equal.

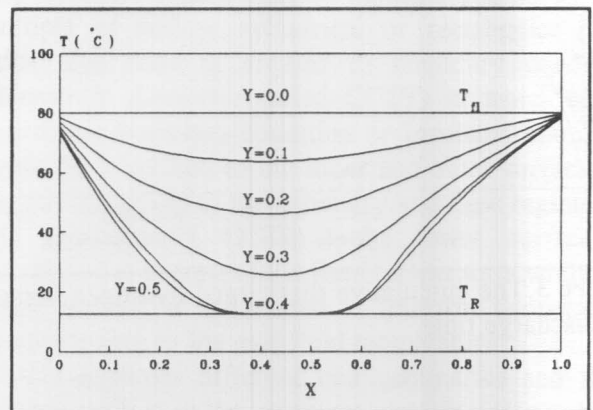


Figure 1. Radial temperature profiles at 90 minutes discharging time and at different dimensionless axial distances.

Figure (2) illustrates the distribution of hydrogen-to-metal atom ratio (H/M) as a function of dimensionless radial distances, X , at mid axial plane ($Y=0.5$) and at different discharging time progress. It is noted that the hydrogen is liberated sequentially from the radial locations which close to the outer and inner surfaces.

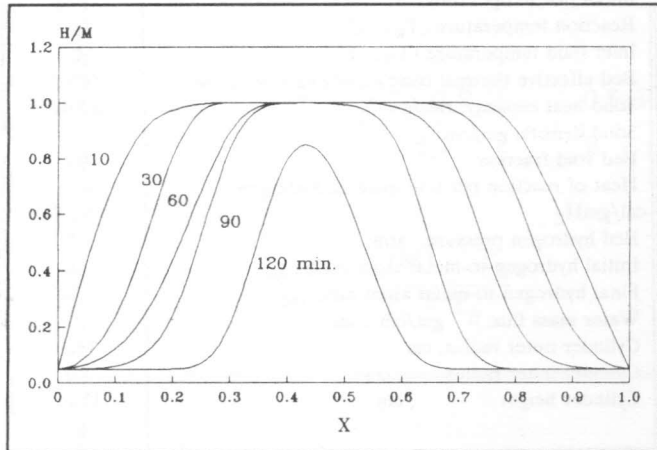


Figure 2. Radial distribution of hydrogen-to-metal atom ratio (H/M) at mid axial plane ($Y=0.5$) and at different discharging time progress.

Figure (3) presents the variation of cumulative discharged hydrogen as the discharge time is progressed. It can be noticed that hydrogen is completely discharged after 136 minutes.

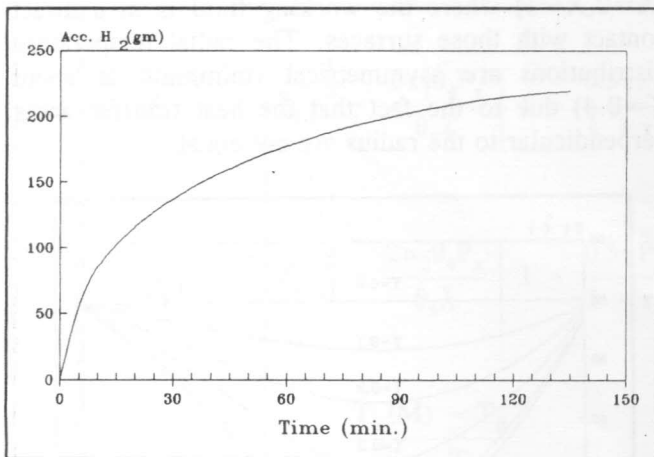


Figure 3. The cumulative discharged hydrogen versus the discharge time.

REFERENCES

- [1] El-Osery, I.A., "A Nuclear Electric-Hydrogen-Energy System", *Energy Journal (Oxford)*, Vol. 9 (8), P. 709-711, 1984, U.K.
- [2] W.S. Yu, E. Suuberg, and C. Waid, "Modelling studies of Fixed-Bed Metal Hydride Storage Systems", in *Hydrogen Energy (Part A)*, Edited by T.N. Veziroglu, Plenum Press, N.Y., U.S.A, p. 621-643, 1975.
- [3] I.A. El-Osery, A.M. Metwally, M.A. El-Osairy and Mayssa A. Hassan, "Towards an Analytical Solution For Heat Transfer Problems in Metal Hydride Conduction Bed Model", *Proceedings of the second Cairo Int. Symposium on Renewable Energy Sources, Cairo-Egypt. 1-4 October, 1990.*
- [4] F.W. Schmidt, A.J. Willmott, "Thermal Energy Storage and Regeneration", *Hemisphere Publishing Co., Washington*, 1981.
- [5] B. Carnahan, H.A. Luther and J.O. Wilkes, "Applied Numerical Methods", *Jhon Wiley & Sons Inc., N.Y.*, 1969.
- [6] A.R. Mitchell, "Computational Methods in Partial Differential Equations", *John Wiley, London*, 1969.
- [7] L.J. Swartzendruber, G.C. Carter, D.J. Kahan, M.E. Read and J.R. Manning, "Numerical Physical Property Data For Metal Hydrides Utilized For Hydrogen Storage", *Hydrogen Energy System. IV*, Edited by T.N. Veziroglu, Pergamon Press, Oxford, England, 1979.